Contents lists available at ScienceDirect

Experimental Cell Research

journal homepage: http://ees.elsevier.com

The Dual Oxidase Duox2 stabilized with DuoxA2 in an enzymatic complex at the surface of the cell produces extracellular H_2O_2 able to induce DNA damage in an inducible cellular model

Louise Poncelet, Jacques-Emile Dumont, Françoise Miot, Xavier De Deken *

Institut de Recherche Interdisciplinaire en Biologie Humaine et Moléculaire (IRIBHM), Université Libre de Bruxelles (ULB), Brussels, Belgium

ARTICLE INFO

Keywords
Duox
DuoxA
Reactive oxygen species
DNA damage
N-glycosylation
Nox

ABSTRACT

Thyroid hormone synthesis requires H_2O_2, produced by two NADPH oxidases, Duox1 and Duox2. To be fully active at the apical pole of the thyrocytes, these enzymes need additional maturation factors DuoxA1 and DuoxA2. The proteins have been shown to be localized at the cell surface, suggesting that they could form a complex with Duox counterparts. We have generated multiple HEK293 Tet-On3G cell lines that express various combinations of DuoxA upon doxycycline induction, in association with a constitutive expression of the Duox enzyme. We compared Duox specific activity, Duox/DuoxA cell surface interactions and the cellular consequences of sustained H_2O_2 generation. By normalizing H_2O_2 extracellular production by Duox or DuoxA membrane expression, we have demonstrated that the most active enzymatic complex is Duox2/DuoxA2, compared to Duox1/DuoxA1. A direct cell surface interaction was shown between Duox1/2 and both DuoxA1 and DuoxA2 using the Duolink® technology, Duox1/DuoxA1 and Duox2/DuoxA2 membrane complexes being more stable than the unpaired ones. A significant increase in DNA damage was observed in the nuclei of Duox2/DuoxA2 expressing cells after doxycycline induction and stimulation of Duox catalytic activity. The maturation and activity of Duox2 were drastically impaired when expressed with the glycosylation-defective maturation factor DuoxA2, while the impact of the unglycosylated DuoxA1 mutant on Duox1 membrane expression and activity was rather limited. The present data demonstrate for the first time that H_2O_2 produced by the Duox2/DuoxA2 cell surface enzymatic complex could provoke potential mutagenic DNA damage in an inducible cellular model, and highlight the importance of the co-expressed partner in the activity and stability of Duox/DuoxA complexes.

Abbreviations

CGD	Chronic Granulomatous Disease
Duox	Dual Oxidase
DuoxA	Duox Activator
EndoH	Endoglycosidase H
ER	Endoplasmic Reticulum
Nox	NADPH Oxidase
PLA	Proximity Ligation Assay
PMA	Phorbol 12-Myristate 13-Acetate
ROS	Reactive Oxygen Species
SOD	Superoxide Dismutase
TH	Thyroid Hormone
TPO	Thyroperoxidase

1. Introduction

The existence of a thyroid H_2O_2-generating system was postulated in the early seventies to be required for thyroid hormone (TH) synthesis by the thyroperoxidase (TPO) enzyme [1]. The Dual Oxidase enzymes, Duox1 and Duox2, are two NADPH oxidases (Nox) belonging to the Nox Family along with Nox 1 to 5 [2,3]. In addition to the conserved Nox catalytic domain, the primary structure of Duox proteins is extended by an NH_2-terminal peroxidase-like ectodomain followed by an additional transmembrane segment and an intracellular loop containing two EF-Hand motifs responsible for their catalytic activation via calcium ions. They are mainly expressed at the apical pole of thyrocytes to allow TPO-mediated iodide organification, but also in the intestine as well as in the respiratory tract, where they play a key role in host defense in association with peculiar peroxidases and thiocyanate [4]. In 2002, the characterization of the first inactivating *Duox2*

* Corresponding author. IRIBHM, Université Libre de Bruxelles, Campus Erasme, Bat. C., 808 route de Lennik, B-1070, Brussels, Belgium.
E-mail addresses: louise.poncelet@ulb.ac.be (L. Poncelet); jedumont@ulb.ac.be (J-E Dumont); fmiot@ulb.ac.be (F. Miot); xdedeken@ulb.ac.be (X. De Deken)

https://doi.org/10.1016/j.yexcr.2019.111620
Received 26 March 2019; Received in revised form 6 September 2019; Accepted 7 September 2019
Available online xxx
0014-4827/

mutations causing iodide organification defect undoubtedly demonstrated the essential role played by Duox2 in TH synthesis [5]. To date, about 105 *Duox2* variants have been described in more than 200 unrelated congenital hypothyroid patients [6]. However, *Duox2* biallelic mutations can be associated with permanent as well as mild transient congenital hypothyroidism, suggesting that Duox1 can partially compensate for the loss of Duox2 [7,8]. Furthermore, the combination of mutations in both *Duox1* and *Duox2* genes has been associated with a more severe phenotype of inherited hypothyroidism [9].

One crucial step for Duox activation is their transition to the cell surface for the production of extracellular hydrogen peroxide. This maturation process is mediated by their respective maturation factors DuoxA1 or DuoxA2 [10]. *Duox* and *DuoxA* genes are arranged in a head-to-head position on the chromosome 15q15.3, allowing co-transcription of both *Duox* and *DuoxA* in the same tissues via bidirectional promoters [11]. DuoxA1 and DuoxA2 proteins were first described as endoplasmic reticulum (ER) resident proteins acting as chaperones for Duox enzymes [10]. However, subsequent studies clearly showed that DuoxA proteins are also detected at the cellular membrane and could therefore form an enzymatic complex with their Duox counterpart [12,13]. The identification of cysteines forming disulfide bridges between Duox and DuoxA proteins supports this hypothesis [14–16]. However, the final proof of their interaction at the surface of the cell is still lacking. Duox exit from the ER can be monitored via sugar modifications by the Golgi apparatus during their maturation processing preceding cell surface incorporation [17]. DuoxA proteins also present *N*-glycosylated putative residues but the role of these sugar modifications on DuoxA function is still unknown [10,12].

As NADPH oxidases, the Duox enzymes should primarily produce superoxide, however when co-expressed with their paired partner, the final product mainly detected is hydrogen peroxide [12]. Using chimeric DuoxA constructs, we previously demonstrated that the NH_2-terminal end of DuoxA2 specifies the type of reactive oxygen species (ROS), H_2O_2 or $O_2^{\cdot-}$, produced by Duox2 [18]. Moreover, the COOH-terminal end of DuoxA1 was shown to be responsible for Duox1-mediated H_2O_2 production. Ueyama et al. identified the first extracellular loop of Duox1 as responsible for the reduction of $O_2^{\cdot-}$ leakage when transferred in Duox2 [19]. As an H_2O_2 producer, Duox expression and activation need to be tightly regulated. Independent studies have suggested that the accumulation of H_2O_2 necessary for TH biosynthesis may promote a mutagenic environment in the thyroid gland [20]. Duox enzymes are obligate calcium-activated NADPH oxidases, but with activities being also modulated through distinct protein kinase phosphorylation pathways [21]. Although micromolar concentrations of phorbol 12-myristate 13-acetate (PMA) were needed to increase Duox1 function, activation of Duox2 is already observed with nanomolar PMA concentrations. Moreover, protein kinase A stimulation by the adenylate cyclase agonist, forskolin, only stimulates Duox1.

In the present work, we generated HEK293 Tet-On3G cell clones expressing Duox enzymes with their paired or unpaired maturation factors. The expression of DuoxA was under the control of the doxycycline inducible promoter, allowing a precise comparison of Duox specific activity as well as Duox/DuoxA cell surface interaction and stability.

2. Material and methods

2.1. Plasmids and mutagenesis

The NH_2-terminal hemagglutinin (HA) epitope-tagged (YPYDVPDYA) human Duox1 (HA-hDuox1-pIRESpuro) and Duox2 (HA-hDuox2-pIRESpuro) were obtained from pre-existing constructs, HA-hDuox1-pcDNA3 and HA-hDuox2-pcDNA3, respectively, described elsewhere [18]. The HA tag was inserted close to the NH_2-extremity of Duox1 and Duox2 between residues 23–24 and 27–28, respectively. Restriction sites were added into either sides of Duox1 (*Not*I and *Bam*HI) and Duox2 (*Not*I) coding sequences before inserting them into the pIRESpuro vector (Clontech Laboratories, CA, USA). The NH_2-terminal V5 epitope-tagged (GKPIPNPLLGLDST) human DuoxA1 (V5-hDuoxA1-pTRE3G), containing cDNA sequence of the DuoxA1 α-isoform described by Morand et al. [12] was generated from the V5-hDuoxA1-HA-pcDNA3 construct. Briefly, a *Bgl*II restriction site was added upstream of V5-hDuoxA1-HA coding sequence, whereas the HA tag was replaced by a stop codon and a *Mlu*I restriction site. The generated sequence was inserted into the pTRE3G vector (Clontech Laboratories, CA, USA). Finally, the NH_2-terminal V5 epitope-tagged human DuoxA2 (V5-hDuoxA2-pTRE3G) was obtained from the hDuoxA2-myc-pcDNA3 pre-existing construct (generously given by Pr. H. Grasberger). The V5 tag was added upstream of the hDuoxA2-myc coding sequence including the *Bgl*II restriction site, and the myc tag was replaced by a stop codon and the *Mlu*I restriction site. The generated sequence was inserted into the pTRE3G vector (Clontech Laboratories, CA, USA). The absence of mutation in all generated constructs was confirmed by sequencing. As previously demonstrated, these tags did not prevent Duox and DuoxA expression and activity [12,14,15,18].

Mutations of all putative glycosylation sites were introduced into DuoxA1 and DuoxA2 sequences in the V5-hDuoxA-pTRE3G plasmids by site-directed mutagenesis using the Quickchange system (Stratagene, CA, USA) in order to replace asparagines by glutamines.

2.2. Cell culture and transfection

HEK293 Tet-On3G cells and COS-7 cells were cultured at 37 °C in a humidified atmosphere with 5% CO_2 and 20% O_2 in Dulbecco's Modified Eagle's Medium (DMEM – Thermo Fisher Scientific, MA, USA) supplemented with 10% FBS, 100 U/ml penicillin, 100 µg/ml streptomycin, 2.5 µg/ml fungizone and 1 mM sodium pyruvate (Thermo Fisher Scientific, MA, USA). Stable transfection of HEK293 Tet-On3G cells with Duox and DuoxA expressing plasmids (HA-hDuox-pIRESpuro and V5-hDuoxA-pTRE3G, respectively) was performed with Xfect Reagent (Clontech Laboratories, CA, USA) following the manufacturer's instructions. After selection with 100 µg/ml geneticin (InvivoGen, CA, USA), 100 µg/ml hygromycin (Thermo Fisher Scientific, MA, USA) and 0.5 µg/ml puromycin (InvivoGen, CA, USA), clonal cells were isolated by limiting dilution. Each clone was routinely assayed by flow cytometry analysis to verify their clonality and monitor possible changes in Duox and DuoxA protein expression. Transient transfection of COS-7 cells was performed with XtremeGENE 9 DNA Transfection Reagent (Roche Life Science, Germany) following the manufacturer's instructions and using 0.5 µg of each Duox or DuoxA expressing vector in addition to 0.125 µg of the rtTA expression plasmid (Clontech Laboratories, CA, USA). One day following transfection, DuoxA expression was induced with doxycycline (2–1000 ng/ml, Sigma-Aldrich, MO, USA).

2.3. Cell lysis and immunoblot analysis

Protein extracts were obtained by cell lysis in a citrate buffer (pH 5.5) containing 20 mM EDTA, 1% Triton X-100 (BioRad, CA, USA) and protease inhibitors (1 µg/ml leupeptin, 60 ng/ml pefabloc, 1 mg/ml pepstatin and Complete Protease Inhibitor Cocktail (Roche Life Science, Germany). Cell lysate was rocked at 4 °C for 1 h and centrifuged at 10,000 g for 10 min to collect the soluble protein fraction. Protein concentrations were determined by the Pierce 660 nm Protein Assay (Thermo Fisher Scientific, MA, USA). Proteins were denatured in Laemmli buffer for 1 min at 80 °C. To analyze Duox maturation, proteins were first treated with endoglycosidase H (EndoH, 5 mU, Roche Life Science, Germany) at 30 °C for 30 min but not heated at 80 °C. Equal amounts (10–30 µg) of proteins were separated on an

SDS/polyacrylamide gel, before being transferred to nitrocellulose (GE Healthcare, IL, USA) or PVDF (Merck Millipore, MA, USA) membranes. Membranes were blocked for 1 h at room temperature in Odyssey Blocking buffer (Li-Cor, NE, USA) and incubated overnight at 4 °C with *anti*-Duox (I2, 1/5000) [2], anti-V5 (1/5000, Thermo Fisher Scientific, MA, USA), anti-actin (1/1000, Sigma-Aldrich, MO, USA) or anti-vinculin (1/200, Clone SPM227, Abcam, United Kingdom) antibodies. Fluorescent secondary antibodies (IRDye 680 and IRDye 800, 1/10,000, Li-Cor, NE, USA) were used for image acquisition with the Odyssey Infrared detection system. Quantification of protein expression was assessed by the Odyssey program. The percentage of Duox mature forms was calculated after subtraction of the background value obtained in the control condition (without doxycycline) as follows: the intensity of the mature form was divided by the sum of the intensities of the mature and immature forms of Duox, multiplied by 100.

To inhibit protein synthesis, HEK293 Tet-On3G cells, treated for 3 days with 1 μg/ml doxycycline, were washed to eliminate doxycycline and treated with 100 μg/ml cycloheximide (CHX, Sigma-Aldrich, MO, USA) for 8, 16, 24 or 32 h. Proteins were extracted and analyzed by Western blot (as previously described). Each condition was compared with CHX non-treated cells.

2.4. Measurement of NADPH oxidase activity

Extracellular H_2O_2 production was measured using the Benard and Brault fluorimetric assay [22], specific for H_2O_2 measurements as previously described [23,24], based on homovanillic acid (3-methoxy-4-hydroxyphenylacetic acid, 0.44 mM, Sigma-Aldrich, MO, USA) fluorescence after its oxidation by horseradish peroxidase (0.1 mg/ml, Sigma-Aldrich, MO, USA) in the presence of H_2O_2. Cells were incubated for 90 min at 37 °C in 1 ml Krebs Ringer Hepes (KRH) medium containing stimulating agents such as ionomycin (2 μM, Sigma-Aldrich, MO, USA), forskolin (10 μM, AG Scientific, CA, USA) or phorbol 12-myristate 13-acetate (PMA, 2–5000 nM, Sigma-Aldrich, MO, USA). H_2O_2 production accumulated in the medium was measured using a Tecan Infinite 200 Pro fluorimeter in 96-well black plates, using excitation and emission filters set at 315 and 425 nm, respectively.

2.5. Flow cytometry

HA-Duox and V5-DuoxA surface expression was assessed by flow cytometry using anti-HA.11 (1/100, Clone 16B12, mouse, BioLegend, CA, USA) and anti-V5 (1/150, mouse, Invitrogen) antibodies as described previously. Briefly, cells were detached with PBS containing 5 mM EDTA/EGTA and incubated at room temperature for 30 min with primary antibodies in PBS-0.1% bovine serum albumin (BSA). After washing steps, cells were incubated for 30 min at 4 °C with anti-mouse secondary antibodies (1/100, Alexa Fluor 488, Thermo Fisher Scientific, MA, USA) and with propidium iodide (3 μg/ml, Sigma-Aldrich, MO, USA) to exclude damaged cells from analysis. 20,000 events/sample were analyzed with a Beckman Coulter cytometer and the mean fluorescence intensity of cell populations was determined by the Cyflogic program. Fluorescence intensities obtained in control conditions (without doxycycline) were subtracted from other values. For detection of intracellular proteins, cells were permeabilized with 0.2% saponin in PBS-0.1%BSA before immunodetection with the primary antibodies.

2.6. Proximity ligation assay (Duolink®, Sigma-Aldrich, MO, USA)

To study protein-protein interactions by the proximity ligation assay, cells were plated on 8-well chamber slides (LabTek chamber slides, Thermo Fisher Scientific, MA, USA) 3–7 days before the experiment. After blocking in HBSS-5% normal horse serum (NHS)-5%BSA for 1 h at room temperature, living cells were incubated with two primary antibodies in HBSS-1%NHS-1%BSA: mouse anti-HA.11 to detect HA-Duox and goat anti-V5 (Novus Biologicals, CO, USA) to detect V5-DuoxA. The fixation step with paraformaldehyde (4%) at 4 °C for 10 min was followed by incubation with secondary antibodies coupled with “plus” (anti-mouse, Sigma-Aldrich, MO, USA) and “minus” (anti-goat, Sigma-Aldrich, MO, USA) DNA probes in HBSS-1%NHS-1%BSA for 1 h at 37 °C. The proximity ligation assay was then performed following the manufacturer's instructions, with a 30 min ligation step at 37 °C, followed by the amplification step for 100 min at 37 °C. The nuclei were stained for 10 min with DAPI (1/40,000) and the slides were mounted with FluorSave (Merck Millipore, MA, USA) and analyzed by an Axio Imager Z1 microscope (Zeiss) at 20x magnification. Per experiment, the number of signals per cell from at least 6 images in each tested condition was measured with the R program. Individual protein expression was detected following the manufacturer's instructions using one single primary antibody (mouse anti-HA.11 or goat anti-V5) and two secondary antibodies (anti-mouse or anti-goat) coupled with “plus” and “minus” DNA probes. The proximity ligation assay was performed as described above. In transient transfection experiments, the percentage of positive COS-7 cells (presenting at least 10 PLA positive signals) from all analyzed cells (DAPI positive) was determined with the Blobfinder program (Duolink) from at least 5 images in each tested condition.

2.7. DNA damage measurement – γH2AX immunostaining

Cells were plated in duplicate on 8-well chamber slides (LabTek chamber slides, Thermo Fisher Scientific, MA, USA) 3 days before the experiment. Duox activity was stimulated by incubating cells for 90 min in KRH medium containing 2 μM ionomycin and 5 μM PMA. To scavenge H_2O_2 or $O_2^{\cdot-}$, the cells were pre-incubated with 500 U/ml catalase (cat, Sigma-Aldrich, MO, USA) or 600 U/ml superoxide dismutase (SOD, Sigma-Aldrich, MO, USA), respectively. After fixation with paraformaldehyde and blocking (PBS, 5% Horse Serum, 0.1% Triton X-100, 0.5% Tween20, 10% BSA), cells were incubated overnight at 4 °C with mouse anti-γH2AX primary antibody (1/1000, Merck Millipore, MA, USA) and for 40 min at room temperature with anti-mouse secondary antibody (1/400, RRX, Jackson ImmunoResearch, PA, USA), as well as DAPI (1/30,000) for nuclei staining. Slides were mounted with Glycergel mounting medium (DAKO, CA, USA) and analyzed with an Axio Imager Z1 microscope (Zeiss) at 40x magnification. Total surface of γH2AX foci signal from 6 to 10 images in each experimental condition was normalized to the total surface of nuclei using ImageJ program (Macro by C. Chevalier, CMMI). Each experiment was performed in duplicate in two independent wells.

2.8. Detection of intracellular reactive oxygen species

HEK293 Tet-On3G cells were incubated for 90 min in KRH medium containing 2 μM ionomycin and 5 μM PMA to stimulate H_2O_2 production by Duox enzymes. The cells were loaded with 5 μM CellROX Green Reagent (Thermo Fisher Scientific, MA, USA). In some experiments, 500 U/ml catalase was included to scavenge H_2O_2. Cells were detached with PBS - 5 mM EDTA/EGTA and an equal size population (20,000 events) was analyzed by flow cytometry.

2.9. Statistical analysis

Statistical analysis was performed using GraphPad Prism 6 for paired or unpaired Student's t-test, conformity test or Mann-Whitney test for non-parametric data. Values are presented as means ± standard error of the mean (SEM), $p < 0.05$ was considered statistically significant (*$p < 0.05$, **$p < 0.01$, ***$p < 0.001$).

3. Results

3.1. A novel cellular model to study duox maturation and interaction with DuoxA

Previously, several groups have studied Duox maturation and activity in heterologous cell systems overexpressing Duox and DuoxA proteins [12,13,18,19]. In the present study, we generated stable cell lines constitutively expressing Duox1 or Duox2 associated with the expression of DuoxA1, the α-splice variant, or DuoxA2 under the control of the doxycycline inducible promoter. These cells allowed us to modulate tightly DuoxA1 or DuoxA2 expression to precisely study Duox1 and Duox2 maturation, activity and cell surface interaction with the maturation factors. To reliably study the surface expressions in intact cells, HA- or V5-tags were inserted at the extracellular NH_2-terminal end of Duox and DuoxA proteins, respectively. Four types of HEK293 Tet-On3G cell lines were generated expressing HA-Duox1 and V5-DuoxA1 (D1DA1), HA-Duox2 and V5-DuoxA2 (D2DA2), HA-Duox1 and V5-DuoxA2 (D1DA2) or HA-Duox2 and V5-DuoxA1 (D2DA1). All the experiments were performed with at least two independent HEK293 Tet-On3G cell clones to consider the variability between individual clones.

Increasing concentrations of doxycycline were used to determine maximal induction of DuoxA proteins and the optimal maturation of Duox enzymes. After 3 days of treatment, DuoxA expression measured by Western blot and flow cytometry directly depended on doxycycline concentration. As previously shown by us and others, the appearance of the mature form of Duox (molecular weight: 190 kDa) via complex oligosaccharide addition in the Golgi apparatus (Fig. 1A) was associated with DuoxA expression and corresponded to Duox and DuoxA cell surface expression (Fig. 1B) [12,17]. After quantification of multiple independent experiments performed with a 72 h induction with 1 μg/ml doxycycline, the Duox most abundant mature form was repeatedly observed for Duox1 in combination with DuoxA1 (77% ± 3; n =

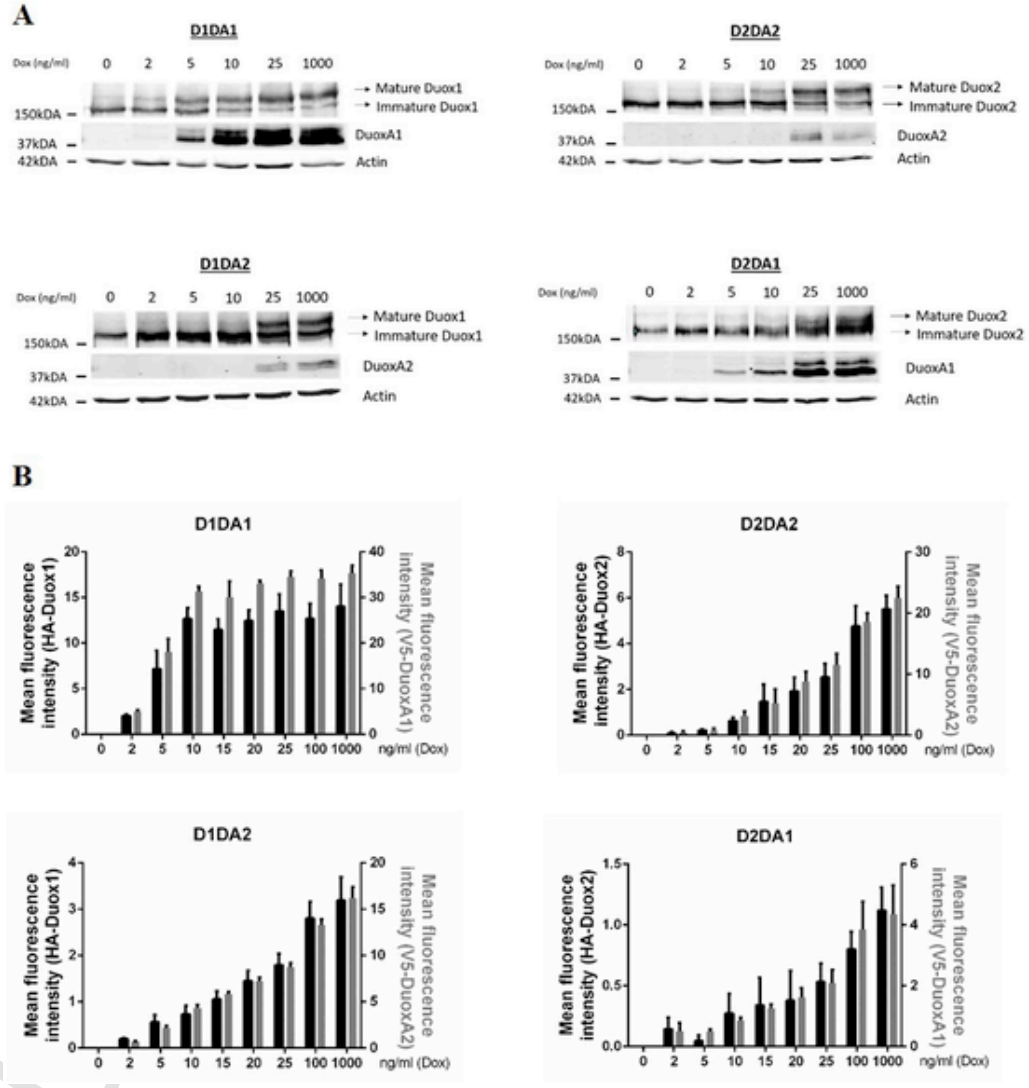

Fig. 1. Duox maturation and surface expression are directly related to DuoxA expression and doxycycline concentrations. HEK293 Tet-On3G clones, expressing Duox1 and DuoxA1 (D1DA1), Duox2 and DuoxA2 (D2DA2), Duox1 and DuoxA2 (D1DA2) or Duox2 and DuoxA1 (D2DA1) were treated for 72 h with increasing concentrations of doxycycline (Dox, 0–1000 ng/ml). (A) Western blot analysis of Duox and DuoxA protein expression and maturation. Fifteen μg of proteins were loaded on polyacrylamide gels and immunoblotted, as described in Material and Methods, after treatment with endoglycosidase H to distinguish expression of mature (190 kDa) and immature (160 kDa) Duox protein. Data are representative of one experiment out of 4 performed with 2 independent HEK293 Tet-On3G clones. (B) Duox and DuoxA surface expression measured by flow cytometry. HA-Duox and V5-DuoxA expressions were detected at the surface of non-permeabilized cells with anti-HA and anti-V5 antibodies. Data are presented as means ± standard error of the mean (SEM) of the mean fluorescence intensity of doxycycline treated cell population minus the mean fluorescence intensity of non-induced cells (without doxycycline) in 3 different experiments and 2 independent Duox/DuoxA clones.

10). DuoxA2 allowed the processing of 59% ± 5 (n = 10) of Duox2 and 48% ± 7 (n = 9) of Duox1. When co-expressed with DuoxA1, 43% ± 4 (n = 9) of the Duox2 mature form could be detected. The correct processing of Duox proteins was correlated with cell surface expressions of both Duox and the maturation factor (Fig. 1B). A maximal Duox/DuoxA cell surface expression was reached for all the combinations after DuoxA induction with 1 μg/ml doxycycline. Time course experiments showed that 24 h of doxycycline treatment was sufficient for optimal Duox maturation, except for Duox2 associated with DuoxA1, which required longer DuoxA induction (data not shown). Based on the flow cytometry experiments, we decided to treat all the cells with 1 μg/ml of doxycycline over 72 h for all the subsequent experiments to compare the different Duox/DuoxA expressing cells reliably.

No extracellular H_2O_2 accumulation was detected in the absence of doxycycline, and very weak basal activity was measured after DuoxA induction (Fig. 2A). Duox-dependent H_2O_2 production (nmol H_2O_2/90 min/100,000 cells; n = 3) was significantly increased after treatment with 2 μM ionomycin (D1DA1: 0.54 ± 0.06, D2DA2: 0.38 ± 0.07, D1DA2: 0.13 ± 0.03, D2DA1: 0.03 ± 0.01), even if the amount of H_2O_2 generated by Duox associated with unpaired maturation factors was very weak. As expected, only Duox1 activity was increased by the adenylate cyclase agonist, forskolin. The combination of ionomycin with forskolin or the PKC activator, PMA, potentiated Duox1 or Duox2 activity, respectively.

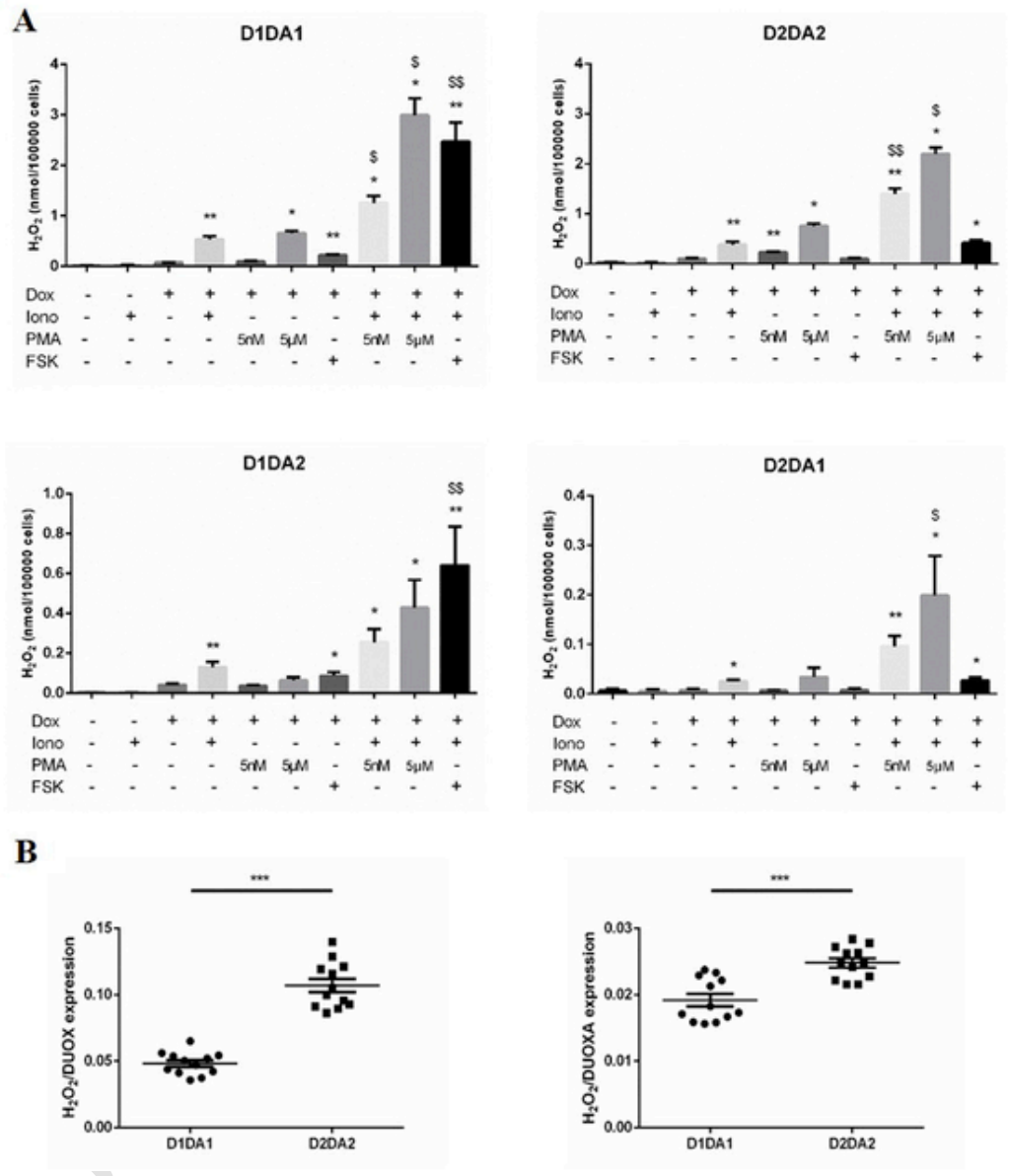

Fig. 2. H_2O_2 production by Duox1 and Duox2 enzymes. (A) H_2O_2 production in response to various stimulating agents. HEK293 Tet-On 3G cells were treated or not during 72 h with 1 μg/ml doxycycline (Dox). H_2O_2 production was measured after 90 min of stimulation with vehicle alone, ionomycin (Iono, 2 μM), PMA (5 nM or 5 μM) or forskolin (Fsk, 10 μM). Data are presented as means ± SEM of at least 3 different experiments on 2 independent HEK293 Tet-On3G clones. Mann-Whitney tests were performed to compare doxycycline-dependent H_2O_2 production of stimulated cells with cells treated with vehicle alone (*$p < 0.05$, **$p < 0.01$, ***$p < 0.001$) or cells stimulated with ionomycin alone ($ $p < 0.05$, $$ $p < 0.01$, $$$ $p < 0.001$). (B) Calcium activated Duox2/DuoxA2 produces more H_2O_2 than Duox1/DuoxA1 when normalized to cell surface expression. HEK293 Tet-On3G clones expressing either Duox1 and DuoxA1 (D1DA1) or Duox2 and DuoxA2 (D2DA2), were treated with 3 different doxycycline concentrations (D1DA1: 2, 5, 10 ng/ml; D2DA2: 15, 20, 25 ng/ml) for 72 h and H_2O_2 production was measured after 90 min stimulation with 2 μM ionomycin. H_2O_2 production was normalized to Duox (left panel) and DuoxA (right panel) cell surface expression determined by flow cytometry. Data were repeated in three different experiments and in 2 independent HEK293 Tet-On3G clones. The means with SEM are presented on the graphs.

3.2. Duox2 enzyme is more active than Duox1

We previously demonstrated a linear correlation between Duox cell surface expression and extracellular H_2O_2 production [21]. In the present heterologous system, using increasing amounts of doxycycline, we confirmed the linear relationship of membrane Duox-dependent H_2O_2 generation as well as of cell surface DuoxA-mediated H_2O_2 production (Supplementary Fig. S1). In addition, thanks to the identical extracellular HA tag, we compared the specific activity of each Duox enzyme in combination with its own maturation factor using three different doxycycline concentrations and after normalization against Duox membrane expression measured by flow cytometry and anti-HA staining (Fig. 2B). We show that the Duox2 oxidase was almost 2 fold more active than Duox1. Moreover, when the H_2O_2 production was normalized to the membrane expression of the maturation factors using the V5 tag, the specific catalytic activity of Duox2 was again significantly higher than that of Duox1.

3.3. Duox and DuoxA stability depends on their co-expressed partner

It is well known that in leukocytes of patients suffering from chronic granulomatous disease (CGD) caused by *CYBA* inactivating mutations, the absence of $p22^{phox}$ protein impairs the correct maturation of the NADPH oxidase Nox2 whose expression is barely detectable, demonstrating the crucial role played by $p22^{phox}$ on Nox2 stability [25]. Recently, it has been shown that DuoxA2 stability is highly dependent on Duox2 oxidative folding through intra-molecular disulfide bridges [14]. We have monitored Duox maturation and activity when DuoxA expression was decreased by washing out doxycycline from the culture medium after the induction period. After 72 h of doxycycline treatment followed by cell washing, Duox and DuoxA protein expression (Fig. 3A and C) and H_2O_2 production (Fig. 3B) were measured during 1, 2, 3 or 4 days without doxycycline. In cells expressing Duox with its paired DuoxA partner, the mature form of Duox remained detectable until 4 days after doxycycline removal. Cell surface expression of both proteins as well as H_2O_2 generation were also maintained 4 days after doxycycline withdrawal; the amount of H_2O_2 produced following the remaining Duox/DuoxA membrane expression. However, in the presence of the cross-functioning maturation factor (D1DA2 and D2DA1 cells) the high molecular weight form of Duox disappeared much faster, associated with barely detected H_2O_2 production and cell surface expression at day 4. The prolonged period of Duox maturation observed days after doxycycline withdrawal could probably be explained by the persistence of rtTA-mediated transcriptional activity and/or residual transcripts being translated.

To precisely evaluate the half-life of Duox and DuoxA proteins, cells were treated (Fig. 4A) or not (Supplementary Fig. S2) with

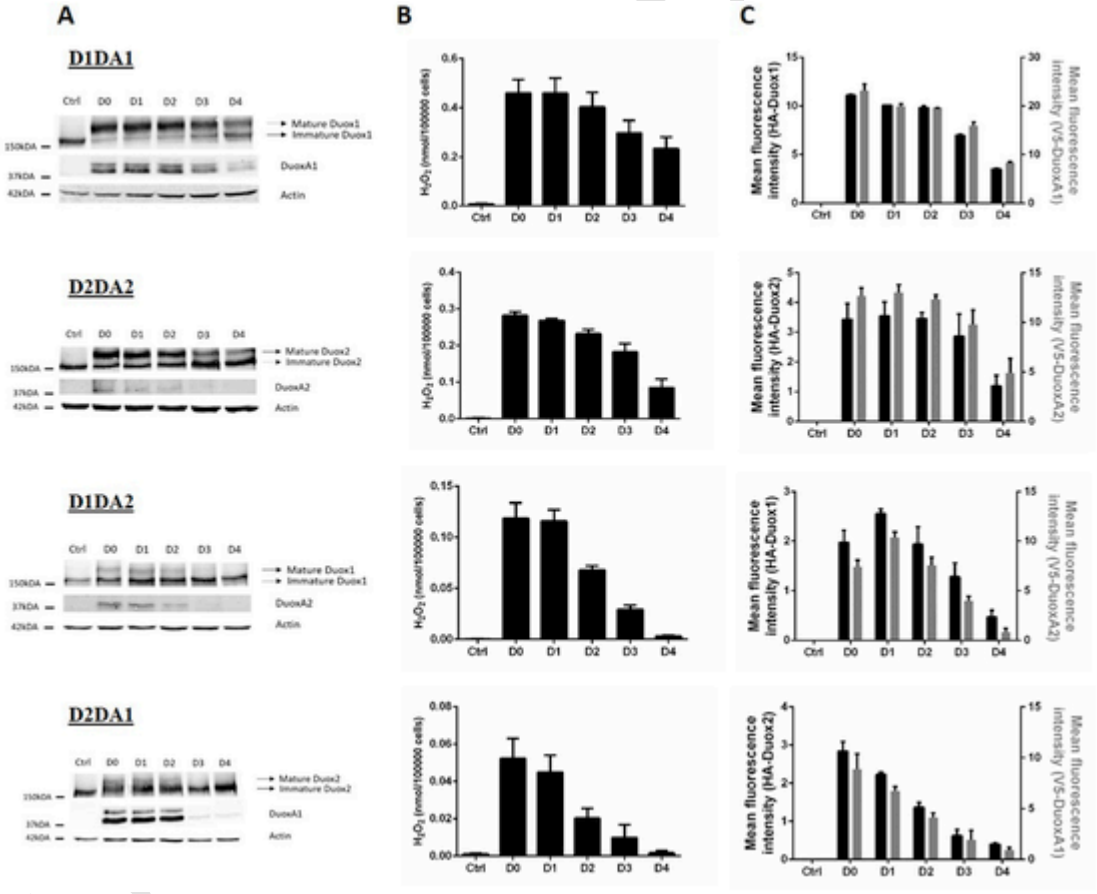

Fig. 3. Duox maturation, activity and cell surface expression persist longer when expressed with its paired maturation factor. HEK293 Tet-On3G clones were treated for 72 h with 1 μg/ml doxycycline (D0) and washed to withdraw doxycycline from the culture medium. Cells were stopped 1, 2, 3 or 4 days after the washing step (D1, D2, D3, D4). Control cells (Ctrl) were not induced with doxycycline and stopped 4 days after the washing step. (A) Fifteen μg of proteins were separated by Western blot after endoglycosidase H treatment to analyze Duox maturation and DuoxA expression. One representative Western blot experiment is presented. (B) H_2O_2 production was measured after 90 min stimulation with 2 μM ionomycin. Data are presented as means ± SEM of 3 different experiments. (C) Duox and DuoxA surface expression measured by flow cytometry. HA-Duox and V5-DuoxA expression were detected at the surface of non-permeabilized cells with anti-HA and anti-V5 antibodies. The mean fluorescence intensity of control cells was subtracted from the mean fluorescence intensity of cells treated with doxycycline. Data are presented as means ± SEM from 3 independent experiments. All experiments (A, B, C) were confirmed on another series of independent Duox/DuoxA clones.

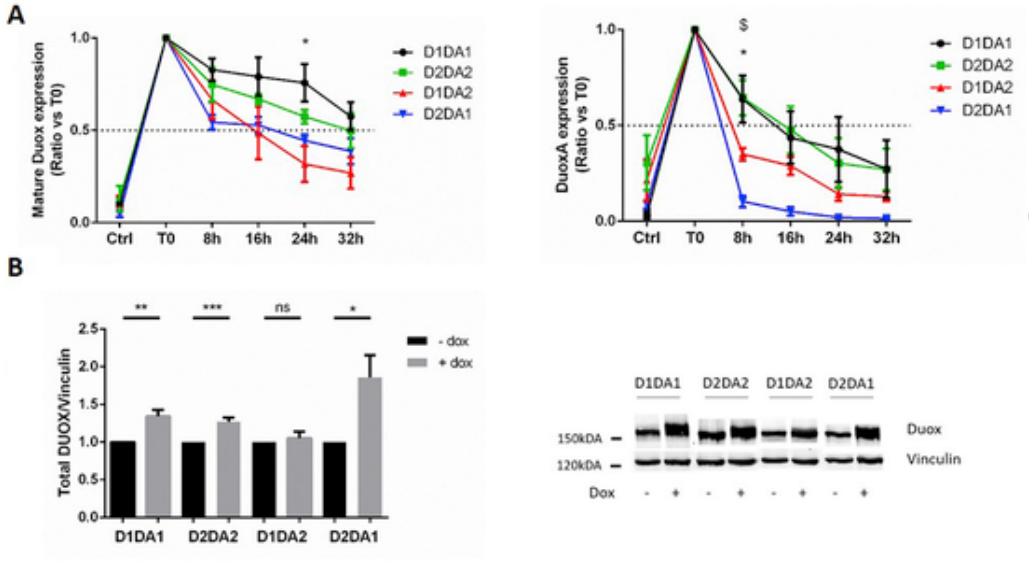

Fig. 4. Duox is stabilized by DuoxA. (A) The half-life of Duox and DuoxA proteins increases in paired complexes. HEK293 Tet-On3G clones expressing different combination of Duox/DuoxA proteins were treated 72 h with 1 μg/ml doxycycline (T0), washed to eliminate doxycycline from the culture medium and cultured with 100 μg/ml cycloheximide. Proteins were extracted after 8, 16, 24 or 32 h and analyzed by Western blot. Control cells (Ctrl) not induced with doxycycline were stopped 32 h after the washing step. The expression of Duox mature protein (EndoH-resistant) was normalized to vinculin and DuoxA expression to actin. Protein expression at T0 was considered as 1. Data are presented as means ± SEM of 3 different experiments in 2 different Duox/DuoxA cell clones. Unpaired Student's t-tests were performed to compare the different values of protein expression. Significant differences were obtained between D1DA1 and D1DA2 after 24 h regarding mature Duox expression (left panel, *$p < 0.05$), and for DuoxA expression between D1DA1 and D2DA1 (right panel, *$p < 0.05$) and between D2DA2 and D1DA2 (right panel, $ $p < 0.05$) after 8 h. (B) The level of Duox protein is increased by DuoxA. HEK293 Tet-On3G clones were treated (grey) or not (black) for 72 h with 1 μg/ml doxycycline. Protein extracts without EndoH treatment of 8 different experiments from two series of independent clones were analyzed by Western blot. Total Duox expression was normalized to vinculin. The values of normalized Duox expression obtained in the non-induced cells were considered as 1. The means ± SEM are presented on the graphs ($n = 8$). One representative Western blot experiment is shown in the right panel.

cycloheximide (100 μg/ml) after induction by doxycycline. In cells expressing Duox with its corresponding maturation factor, the half-life was about 32 h and 16 h for the mature oxidase and the DuoxA protein, respectively. However, in the presence of unpaired DuoxA the half-life of both proteins seems to drop to about 16 h for mature Duox and less than 8 h for the maturation factor, suggesting the importance of the paired partners for the stability of Duox/DuoxA complexes. Finally, by analyzing the total level of Duox expression (without endoglycosidase H treatment), we observed that DuoxA expression could significantly increase the total amount of the oxidase, except in Duox1/DuoxA2 expressing cells (Fig. 4B). These data confirm our previous observation obtained with DuoxA chimeras showing that Duox1 was more dependent than Duox2 on its dedicated maturation factor [18].

3.4. Duox/DuoxA form cell surface complexes that are more stable with paired partners

Previous studies using immunofluorescence staining clearly showed the cell surface expression of Duox and DuoxA proteins [12,13]. Indirect methods based on immunoprecipitation experiments suggested also that these two proteins interact at the membrane via extracellular domains [14,16]. However, the final proof of Duox interaction with its maturation factor at the cell surface is still lacking. We used the proximity ligation assay (PLA, Duolink® technology) to specifically detect the protein-protein surface interaction by staining living cells with corresponding anti-HA and -V5 primary antibodies before the fixation step. We also evaluated the presence of these complexes over time in our four different cell lines (D1DA1, D2DA2, D1DA2 and D2DA1) after doxycycline withdrawal. We first verified that the signal observed was specific for the cell surface by detecting the membrane expression of Duox or DuoxA proteins by PLA (Supplementary Fig. S3). A positive PLA signal for Duox expression was detected only after doxycycline-mediated induction of DuoxA expression, even if Duox proteins were constitutively expressed inside the cells (Supplementary Figs. S3A and B). Furthermore, no DuoxA membrane expression could be detected in HEK293 Tet-On3G cells expressing only DuoxA1 or DuoxA2 after doxycycline treatment (Supplementary Fig. S3C). After a 72 h treatment with 1 μg/ml doxycycline (D0), we clearly observed a positive PLA interaction signal in all HEK293 Tet-On3G cell lines (Fig. 5). The signal was weaker when Duox2 and DuoxA1 were co-expressed, in correlation with a lower cell surface expression (Fig. 1B). Quantification of the number of dots per cell by the R program confirmed the lower level observed in D2DA1 clones (D1DA1: 30 ± 3 signals/cell, D2DA2: 32 ± 3 signals/cell, D1DA2: 24 ± 2 signals/cell, D2DA1: 16 ± 2 signals/cell; $n = 3$). Three days after doxycycline withdrawal (D3), the Duox/DuoxA membrane interaction was maintained in D1DA1 and D2DA2 cells, but the PLA signal significantly dropped in cells expressing cross-functioning partners, suggesting that complexes composed of paired Duox/DuoxA proteins were more stable at the cell surface than unpaired complexes. We verified that these Duox/DuoxA interactions were specific by co-expressing V5-DuoxA and untagged-Duox (to ensure DuoxA cell surface expression) with unrelated HA-tagged proteins (the receptor of the chemokine chemerin (ChemR23) and the atypical chemokine receptor D6 [26,27]). No significant PLA interaction signal was detected, although the corresponding proteins were correctly addressed at the cellular membrane (Supplementary Fig. S4).

3.5. Glycosylation of DuoxA is needed for Duox and DuoxA surface expression and duox activity

DuoxA1 and DuoxA2 are also *N*-glycosylated proteins presenting respectively 4 and 3 putative sites of glycosylation (Fig. 6A) [10]. However, the additional putative *N*-linked glycosylation target residue Asn-71 of DuoxA1 is located at the end of the second transmembrane domain, suggesting that it might not be modified. It has been shown that glycosylation-defective mutants of Duox enzymes are unable to be

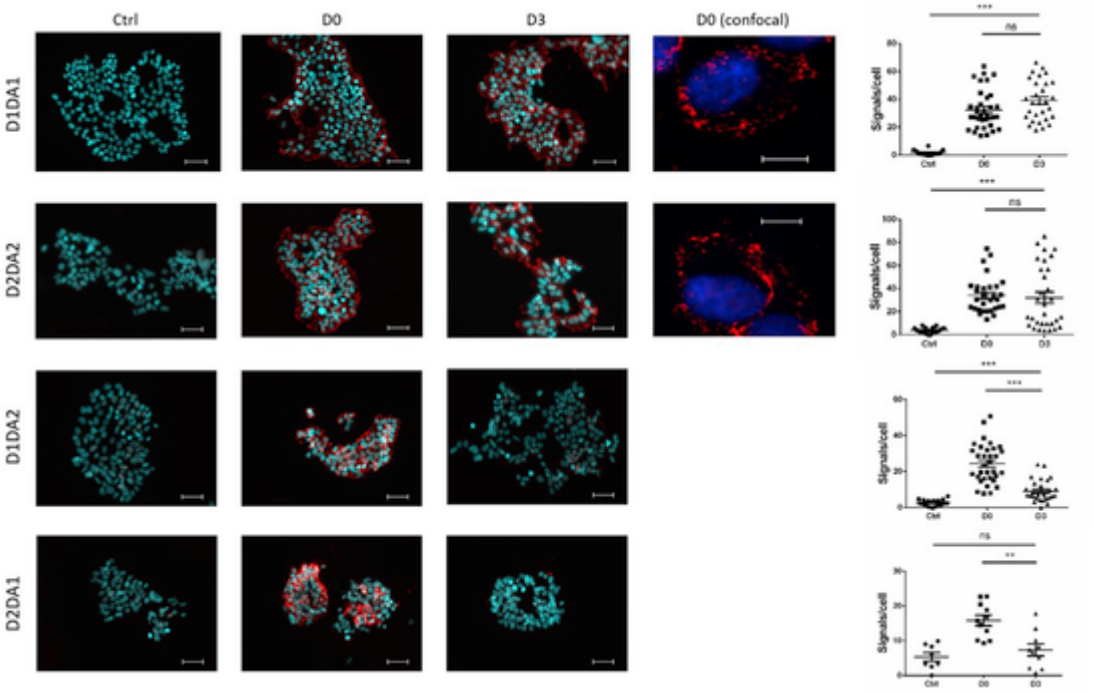

Fig. 5. Cell surface interaction between Duox and DuoxA persists longer in cells expressing matched Duox/DuoxA partners. HEK293 Tet-On3G were treated (D0) or not (Ctrl) during 72 h with 1 μg/ml doxycycline. The medium was changed to withdraw doxycycline and cells were stopped 3 days after the washing step (D3). Duox/DuoxA surface interaction was detected on non-permeabilized cells using the PLA technology (red signal) as described in Material and Methods. The nuclei were stained with DAPI (blue). Scale bars: 50 μm. Images on the right (D0 confocal) were obtained by confocal microscopy (LSM 510 Meta (Zeiss)). Scale bars: 10 μm. The number of positive PLA signals per cell from 3 independent experiments was plotted on the graph for each experimental condition. The means ± SEM are presented. Results were confirmed on another series of independent Duox/DuoxA clones. (For interpretation of the references to colour in this figure legend, the reader is referred to the Web version of this article.)

correctly processed at the cell surface, resulting in the absence of H_2O_2 production [19]. To evaluate whether glycosyl modifications of DuoxA could affect their function in relation to Duox processing and activity, all putative glycosylation sites (Asn-71, Asn-84, Asn-109, Asn-121 in DuoxA1 and Asn-84, Asn-109, Asn-121 in DUOXA2) were replaced by glutamines (Gln) using site-directed mutagenesis. The corresponding mutant constructs were transiently transfected in COS-7 cells with Duox expressing plasmids and DuoxA expression was induced by 1 μg/ml doxycycline during 72 h. The DuoxA variants presented faster electro-mobility shift (Fig. 6B). The maturation of Duox2 was dramatically impaired when expressed with its glycosylation-defective maturation factor, while the mature form of Duox1 was still present even if the expression was slightly reduced. Cell surface expression of the Duox2 and DuoxA2 mutants were also drastically diminished, with very low H_2O_2 produced (Fig. 6C and D). However, the impact of impaired glycosylation on the DuoxA1 mutant remained limited, on its cell surface expression, as well as on Duox1 membrane expression and activity (Fig. 6C and D).

3.6. Hydrogen peroxide produced by active Duox2/DuoxA2 complex can induce DNA damage

Hydrogen peroxide is able to provoke DNA single and double strand breaks and is involved in RET/PTC1 rearrangements in human thyroid cells, suggesting that hormonogenic H_2O_2 could participate to the high rate of spontaneous mutations observed in the thyroid tissue [28–33]. Using histone H2AX phosphorylation (γH2AX) immunostaining, we investigated the impact of the H_2O_2 produced by Duox/DuoxA cell lines on DNA damage. After 90 min of Duox2-mediated H_2O_2 accumulation by stimulation with 2 μM ionomycin and 5 μM PMA, we showed a clear increase of γH2AX signals in Duox2/DuoxA2 expressing cells (Foci surface/Nuclei surface: 37.2% ± 1.3; n = 3) (Fig. 7A). Treatments with catalase, a scavenger of H_2O_2, but not with superoxide dismutase, protected DNA from double strand breaks in these Duox2/DuoxA2 expressing cells. Similar results were obtained by Western blot (Supplementary Fig. S5) and in two additional independent HEK293 Tet-On3G cell lines expressing Duox2 and DuoxA2 (Supplementary Fig. S6). The amount of DNA damage was dependent on the level of Duox2 activity and a significant increase of γH2AX foci could be measured already after 15 min of Duox2 stimulation in cells incubated with ionomycin and PMA (Fig. 7B and C). No augmentation of γH2AX foci could be detected in all other investigated HEK293 Tet-On3G cell clones or without induction of DuoxA expression by doxycycline (Supplementary Fig. S7). Surprisingly, γH2AX foci could not be detected in Duox1/DuoxA1 cells after stimulation of 90, 120 or 180 min, while in these cells external H_2O_2 added to the medium still provoked the expected DNA damage (Supplementary Figs. S5 and S7).

To monitor the intracellular ROS accumulation upon Duox2 activation, we used the CellROX fluorogenic probe that exhibits a strong fluorescent signal upon oxidation. An increase in the fluorescence intensity was observed in Duox2/DuoxA2 expressing cells stimulated with 2 μM ionomycin and 5 μM PMA only after doxycycline induction (Fig. 8), while incubation with catalase significantly diminished the level of intracellular ROS. No such modulation of intracellular ROS was observed in the other investigated Duox/DuoxA cell lines (Supplementary Fig. S8).

4. Discussion

In the present work, DuoxA inducible cell lines were generated to study Duox expression, activity and interaction with regard to the presence of the maturation factor. This inducible system offered for the first time the possibility to characterize the temporal relationship between the oxidase and the maturation factor better. In order to circumvent

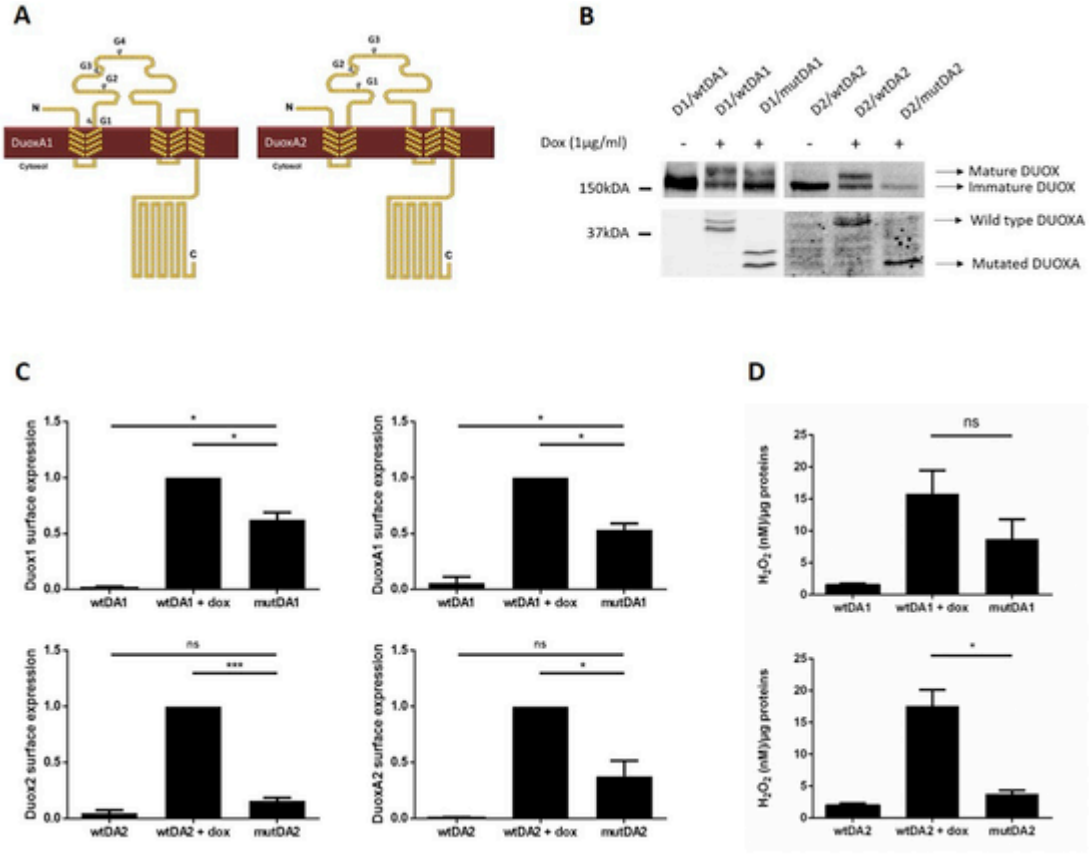

Fig. 6. *N*-glycosylation of DuoxA is needed for Duox expression and activity. COS-7 cells were co-transfected with plasmids expressing Duox1 or Duox2, and wild type (wt) or mutated (mut) DuoxA. After 72 h of treatment with 1 µg/ml doxycycline, cells were harvested for analysis of protein expression and activity. (A) Schematic representation of DuoxA1 and DuoxA2 with the putative glycosylation sites. (B) Equal amounts of protein were immunoblotted to analyze Duox protein maturation (after EndoH treatment) and DuoxA protein expression (without EndoH treatment). (C) Surface expression of Duox and DuoxA was quantified with PLA technology (one primary antibody) and Blobfinder software. Duox and DuoxA expression in the presence of wild type DuoxA and doxycycline induction was considered as 1. (D) H_2O_2 production was stimulated with 2 µM ionomycin for 90 min and normalized to the total protein content. Data are presented as means ± SEM of 4 independent experiments.

the possible toxic effects of sustained H_2O_2 generation, the function of the Duox enzymes, constitutively expressed in the cells, was switched off until the induction of DuoxA upon doxycycline treatment. All the possible combinations (D1DA1, D2DA2, D1DA2 and D2DA1) have been investigated to decipher better the functional impact of cross-functioning pairs that could be present in epithelial cells where the two Duox/DuoxA isoforms coexist as in the thyroid [20].

Despite the high sequence similarity between Duox1 and Duox2 (83%), the two oxidases present multiple differences in terms of expression and activation mechanisms [20]. In our co-transfected HEK293 Tet-On3G cell lines, we confirmed that the Duox1 enzyme was stimulated upon cAMP cascade activation, whereas Duox2-dependent H_2O_2 generation was increased by nanomolar concentrations of PMA as in heterologous systems transiently expressing Duox and DuoxA [21]. The fundamental role played by DuoxA proteins is to promote the correct maturation of Duox enzymes for their ER exit to the cell surface. Evaluation of the amount of Duox mature forms showed that, as expected, optimum Duox maturation was observed in matched Duox/DuoxA pair expressing cells that provide more than 50% of proteins presenting Golgi-based carbohydrate modifications. Higher cell surface expression of both Duox/DuoxA proteins and H_2O_2 generation were also measured in these cells. The activity of Duox1 and Duox2 is dictated by specific regions of DuoxA1 and DuoxA2, respectively, that also influence their processing and transfer to the cellular membrane [18]. The role played by DuoxA, if not identical, presents similarities with the function of the protein $p22^{phox}$ in association with the other NADPH oxidase, NOX2. Truncated mutants of $p22^{phox}$ have shown that carbohydrate modifications, cell surface expression and enzymatic function of NOX2 are closely related and depend on specific regions of $p22^{phox}$ [34].

DuoxA was suggested to be part of the quality control system. Mutant Duox2 presenting an oxidative folding defect showed protein turnover increased in the presence of DuoxA2 [35]. In the present work, we demonstrated that the steady-state level of Duox proteins was increased after DuoxA induction except for Duox1 co-expressed with DuoxA2. Moreover, in cells expressing matched Duox and DuoxA partners, the half-life of the proteins was estimated at 32 h and 16 h respectively, and significantly dropped in cells expressing unmatched pairs. Stabilization of DuoxA in the presence of Duox was recently demonstrated, highlighting a new facet of the relationship between the two partners. While DuoxA1 was stabilized in the presence of Duox1 or Duox2, only Duox2 increased the expression level of DuoxA2 [14,15]. In conclusion, Duox1 and DuoxA2 may not stabilize each other, resulting in a relatively inefficient enzymatic complex with very low level of cell surface expression [12,18]. Inter-molecular disulfide bonds have been suggested to be involved in the interaction between Duox and DuoxA [14,15]. The respective conformations of Duox1 and DuoxA2 might be incompatible for the formation of such disulfide bridges, limiting the formation of stable complexes. Using DuoxA variants with all the putative *N*-glycosylation sites mutated, we revealed additional functional differences between the two maturation factors. The maturation and activity of Duox2 were dramatically impaired with the glycosylation-defective DuoxA2 mutant, although we cannot exclude the possibility that these mutations could also modify the conformation of the maturation factor limiting the function of the enzymatic

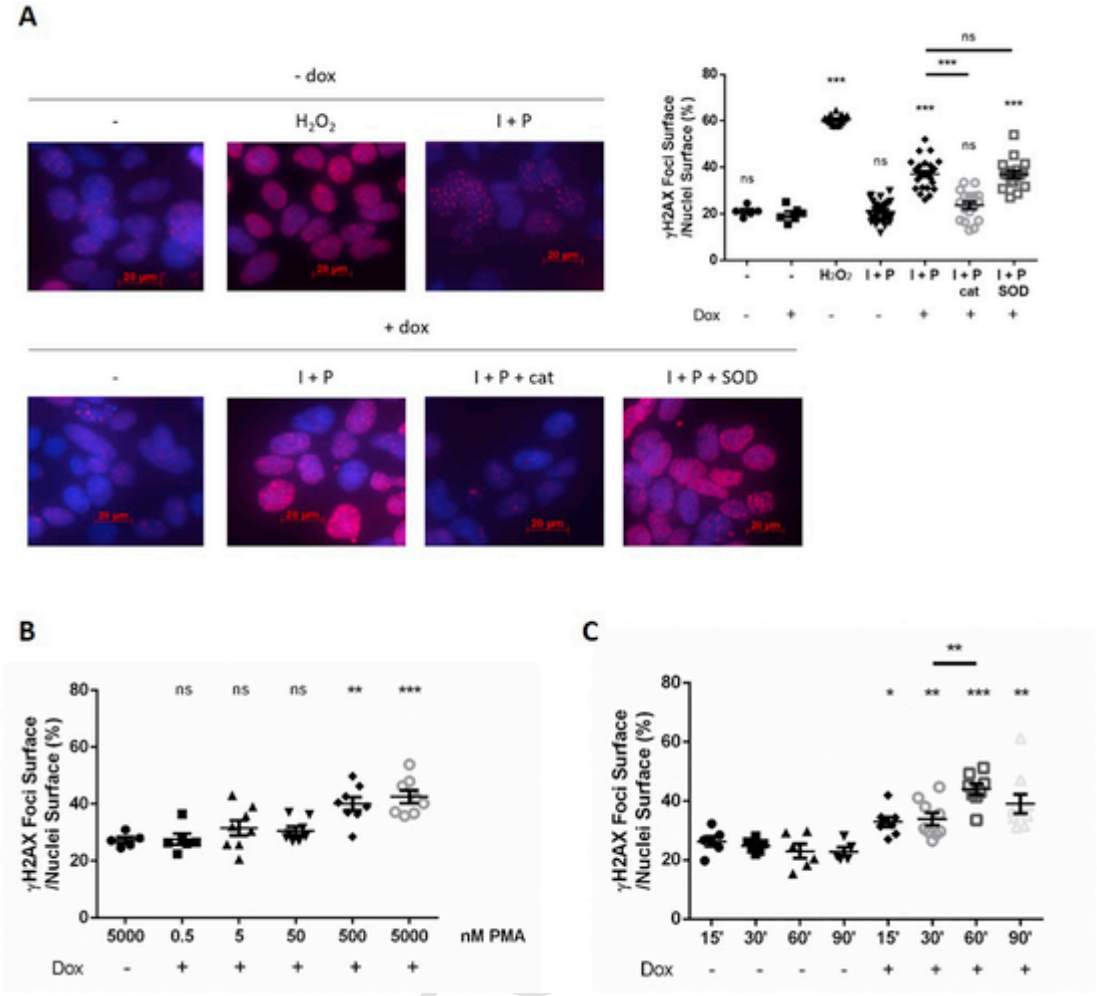

Fig. 7. H_2O_2 produced by Duox2/DuoxA2 expressing cells induces DNA damage. HEK293 Tet-On3G clones (D2DA2) were treated (+Dox) or not (- Dox) during 72 h with 1 μg/ml doxycycline, then incubated for 90 min with stimulating agents (PMA and ionomycin). Cells were fixed and stained for γH2AX foci (red) and DNA (DAPI; blue). Data are presented as the percentage of the surface of γH2AX foci versus the total nucleus surface for each analyzed image. The means ± SEM are presented on the graphs. (A) Cells were incubated with 0.2 mM H_2O_2, 2 μM ionomycin (I), 5 μM PMA (P), 500 U/ml catalase (cat) or 600 U/ml superoxide dismutase (SOD) (n = 3). One representative image of each condition is presented. Scale bars: 20 μm. (B) Cells were incubated with 2 μM ionomycin and increasing amounts of PMA (0.5–5000 nM). (C) Time course analysis of γH2AX foci in cells incubated with 2 μM ionomycin and 5 μM PMA for 15, 30, 60 or 90 min. Statistical significances are presented for each doxycycline condition compared to its corresponding non-induced condition. (For interpretation of the references to colour in this figure legend, the reader is referred to the Web version of this article.)

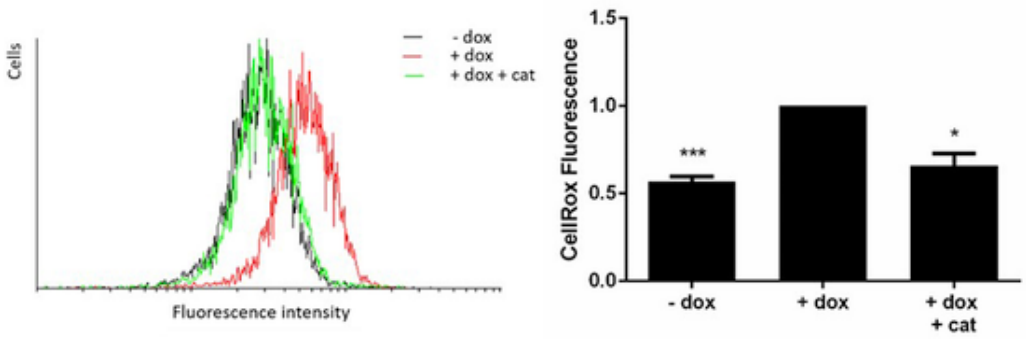

Fig. 8. Detection of intracellular ROS. HEK293 Tet-On3G cells expressing Duox2 and DuoxA2 were treated (+dox) or not (- dox) with 1 μg/ml doxycycline for 72 h. Duox2 activity was stimulated during 90 min with 2 μM ionomycin and 5 μM PMA in the presence or not of 500 U/ml catalase (cat). CellROX signal was analyzed by flow cytometry (n = 3). Condition corresponding to doxycycline treated cells was considered as 1 and conformity test was performed to compare with the other conditions.

complex. The impact of the unglycosylated DuoxA1 mutant on Duox1 membrane expression and activity was rather limited. The putative *N*-glycosylation sites are located in the first extracellular loop of DuoxA proteins where the cysteine 167 of DuoxA2 involved in the inter-molecular disulfide bond with Duox2 is also found. Furthermore, the most frequent DuoxA2 mutation involved in congenital hypothyroidism (p.Y138X) is also located in this extracellular loop, supporting that this region could play a crucial role in the partnership with Duox2 [6].

Direct interaction of the p22^{phox} protein with Nox1-4 is crucial for the formation of a functional oxidase [36,37]. After the discovery that Duox activators not only promote Duox maturation but are also transported to the cell surface, it has been suggested that they could be part of the functional H_2O_2 generating complex with their Duox counterpart [12,13]. Immunoprecipitation experiments have shown interactions between paired Duox/DuoxA proteins, while a much weaker interaction was detected between the cross-functioning partners [12,14,15]. Using the Duolink® technology combined with an adapted protocol, we explored the association of Duox with DuoxA specifically at the cell surface, the correct localization for the active enzyme. Cells expressing matched Duox/DuoxA proteins demonstrated a PLA signal remaining longer compared to Duox1/DuoxA2 and Duox2/DuoxA1, which strongly suggests that DuoxA could have functional implications in the active enzymatic complex. In addition, the linear relationship between the level of extracellular H_2O_2 production and the amount of DuoxA membrane expression also supports this hypothesis. Depending on the enzymatic complex formed, it has been shown that the activity of Duox1 is reduced in the presence of DuoxA2, while superoxide leakage is detected when Duox2 is associated with DuoxA1 [12,18]. The NH_2-extremity of DuoxA and the first extracellular loop of Duox have been demonstrated to be involved in the type of ROS generated by the oxidase [18,19]. Additional experiments are required to define the molecular mechanisms involved in the activation of the enzymatic complex, in particular the different conformations adopted by the proteins depending on the associated maturation factor.

We have demonstrated that the most efficient enzymatic complex in this cellular model is Duox2/DuoxA2 compared to Duox1/DuoxA1, although we cannot ignore the risk that the tag insertion at the NH_2-extremity of the proteins may modify their natural behavior. Even if the thyroid tissue expresses both H_2O_2 generator systems, only biallelic mutations in the *Duox2* gene are responsible for congenital hypothyroidism [6]. The lower specific activity of Duox1/DuoxA1 complex could not be sufficient to compensate for the complete loss of Duox2, especially during the neonatal period where the requirement of thyroid hormones is crucial [38]. However, the transient nature of hypothyroidism observed in some patients carrying biallelic nonfunctional Duox2 variants suggests that Duox1/DuoxA1 may compensate for the defect of Duox2 after the infantile period.

It has been suggested that the high rate of spontaneous mutations observed in the thyroid could be the consequence of the elevated level of H_2O_2 required for TH biosynthesis [20]. Hydrogen peroxide is relatively stable and can freely diffuse through cellular membranes or via channels like aquaporins 3 and 9 [39,40]. We have previously shown that exogenous H_2O_2 can induce DNA single and double strand breaks in human thyrocytes [30,33,41]. Recently, it has been shown that irradiation of a human thyroid cell line induces Duox1-dependent H_2O_2 production provoking persistent DNA damage [29]. We have proposed that a chronic exposure to H_2O_2 generated in the thyroid tissue could, in particular pathological conditions (iodide- or antioxidant-deficiency), be mutagenic promoting benign or malignant tumor formation [32]. For the first time, we provide evidence that H_2O_2 generated by the most potent thyroid oxidase, the Duox2/DuoxA2 complex, is also able to provoke DNA damage in an artificial HEK293 cellular model: 1) Increased of γH2AX foci, mark of DNA damage response, was observed only in doxycycline-induced Duox2/DuoxA2 stimulated cells; 2) The number of γH2AX foci depended on the level of Duox2 activation and duration; 3) Scavenging ROS by catalase, but not superoxide dismutase, prevented DNA damage; 4) Intracellular ROS accumulation was observed only in Duox2/DuoxA2 cells upon Duox2 activation. However, the HEK293 cells are not thyrocytes, which are particularly protected against H_2O_2-induced DNA damage. Multiple factors contributing to the resistance of thyrocytes to hydrogen peroxide have been identified [41]. On the contrary, the HEK293 cells are known to be particularly sensitive to the toxic effects of H_2O_2 [42]. Additional experiments are required to characterize the Duox-mediated DNA damage in a more physiological system like thyrocytes; however treatments with drugs to sensitize the cells to oxidative stress (e.g. buthionine sulphoximine to deplete cells of glutathione) will be most probably required.

The absence of DNA damage increase observed in Duox1/DuoxA1 cells, wherein H_2O_2 production was stimulated, was very surprising. However, these unexpected data do not exclude that H_2O_2-produced by Duox1/DuoxA1 complex could also cause DNA damage in other experimental conditions. Cells expressing Duox1/DuoxA1 produced a similar level of extracellular H_2O_2 (75 nM/90 min/μg proteins) as Duox2/DuoxA2 cells, which was equivalent to the amount generated by primo-cultured human thyrocytes (100 nM/90 min/μg proteins) (Personal communication). However, we demonstrated that the specific activity of the Duox1 enzyme is lower than Duox2, which might not be sufficient for suitable local accumulation of H_2O_2 close to the membrane that may facilitate its passage in the cell to generate cytotoxic effects. In addition, different cellular localizations of the oxidases could also be involved in these discrepancies. Accumulation of multiple Duox2/DuoxA2 enzymatic complexes in microdomains at the cell surface like in lipid rafts could also promote a local concentration of H_2O_2 that would be adequate to reach the critical concentration to induce DNA damage [43]. A nuclear localization of DuoxA1 has been reported in neuronal stem cells [44], however no such nuclear localization for Duox or DuoxA proteins overexpressed in HEK293 cells has been described by us or others [12]. Duox2/DuoxA2 interaction or co-localization with other proteins, like aquaporins, could be also another hypothesis to explain the discrepancy between Duox2 and Duox1-mediated DNA damage, by promoting intracellular H_2O_2 passage.

In conclusion, the present data demonstrated for the first time that the most active cell surface enzymatic complex is Duox2/DuoxA2 and that potential mutagenic DNA damage could be induced in HEK293 cells by hydrogen peroxide generated by this NADPH oxidase. These results highlighted also the importance of the partner in the activity and stability of Duox/DuoxA complexes and raised the question of their functional impact in tissues co-expressing the two Duox/DuoxA isoforms such as the thyroid.

Author disclosure statement

The authors declare that there is no conflict of interest.

Acknowledgments

We thank Chantal Degraef, Sang Tran Van and Bernadette Bournonville for their excellent technical assistance. We kindly thank Clément Chevalier (CMMI, Gosselies) for γ-H2AX foci quantification and Joel Rodrigues Vitória (IRIBHM, ULB) for PLA signal quantification. We are grateful to Dr. H. Grasberger for providing the Duox and DuoxA constructs. We thank J.M. Vanderwinden and the LiMIF facility for the technical support for microscope imaging. This work was supported by the "Fonds de la Recherche Scientifique" (FRS-FNRS; grant number J.0070.16), the Fund Doctor J.P. Naets, managed by the King Baudouin Foundation and the "Foundation Rose et Jean Hoguet".

Appendix A. Supplementary data

Supplementary data to this article can be found online at https://doi.org/10.1016/j.yexcr.2019.111620.

References

[1] J.E. Dumont, The action of thyrotropin on thyroid metabolism, Vitam. Horm. 29 (1971) 287–412, doi:10.1016/S0083-6729(08)60051-5.
[2] X. De Deken, D. Wang, M.-C. Many, S. Costagliola, F. Libert, G. Vassart, J.E. Dumont, F. Miot, Cloning of two human thyroid cDNAs encoding new members

of the NADPH oxidase family, J. Biol. Chem. 275 (2000) 23227–23233, doi:10.1074/jbc.M000916200.
[3] C. Dupuy, R. Ohayon, A. Valent, M.-S. Noël-Hudson, D. Dème, A. Virion, Purification of a novel flavoprotein involved in the thyroid NADPH oxidase, J. Biol. Chem. 274 (1999) 37265–37269, doi:10.1074/jbc.274.52.37265.
[4] M. Geiszt, J. Witta, J. Baffi, K. Lekstrom, T.L. Leto, Dual oxidases represent novel hydrogen peroxide sources supporting mucosal surface host defense, FASEB J. 17 (2003) 1502–1504, doi:10.1096/fj.02-1104fje.
[5] J.C. Moreno, H. Bikker, M.J.E. Kempers, P. van Trotsenburg, F. Baas, J.J.M. de Vijlder, T. Vulsma, C. Ris-Stalpers, Inactivating mutations in the gene for thyroid oxidase 2 (THOX2) and congenital hypothyroidism, N. Engl. J. Med. 347 (2002) 95–102, doi:10.1056/NEJMoa012752.
[6] M. Muzza, L. Fugazzola, Disorders of H_2O_2 generation, Best Pract. Res. Clin. Endocrinol. Metabol. 31 (2017) 225–240, doi:10.1016/j.beem.2017.04.006.
[7] C. Hoste, S. Rigutto, G. Van Vliet, F. Miot, X. De Deken, Compound heterozygosity for a novel hemizygous missense mutation and a partial deletion affecting the catalytic core of the H_2O_2-generating enzyme DUOX2 associated with transient congenital hypothyroidism, Hum. Mutat. 31 (2010) 1304–1318, doi:10.1002/humu.21227.
[8] Y. Maruo, H. Takahashi, I. Soeda, N. Nishikura, K. Matsui, Y. Ota, Y. Mimura, A. Mori, H. Sato, Y. Takeuchi, Transient congenital hypothyroidism caused by biallelic mutations of the dual oxidase 2 gene in Japanese patients detected by a neonatal screening program, J. Clin. Endocrinol. Metab. 93 (2008) 4261–4267, doi:10.1210/jc.2008-0856.
[9] Z. Aycan, H. Cangul, M. Muzza, V.N. Bas, L. Fugazzola, V.K. Chatterjee, L. Persani, N. Schoenmakers, Digenic DUOX1 and DUOX2 mutations in cases with congenital hypothyroidism, J. Clin. Endocrinol. Metab. 102 (2017) 3085–3090, doi:10.1210/jc.2017-00529.
[10] H. Grasberger, S. Refetoff, Identification of the maturation factor for dual oxidase: evolution of an eukaryotic operon equivalent, J. Biol. Chem. 281 (2006) 18269–18272, doi:10.1074/jbc.C600095200.
[11] C. Christophe-Hobertus, D. Christophe, Delimitation and functional characterization of the bidirectional THOX-DUOXA promoter regions in thyrocytes, Mol. Cell. Endocrinol. 317 (2010) 161–167, doi:10.1016/j.mce.2010.01.001.
[12] S. Morand, T. Ueyama, S. Tsujibe, N. Saito, A. Korzeniowska, T.L. Leto, Duox maturation factors form cell surface complexes with Duox affecting the specificity of reactive oxygen species generation, FASEB J. 23 (2009) 1205–1218, doi:10.1096/fj.08-120006.
[13] S. Luxen, D. Noack, M. Frausto, S. Davanture, B.E. Torbett, U.G. Knaus, Heterodimerization controls localization of Duox-DuoxA NADPH oxidases in airway cells, J. Cell Sci. 122 (2009) 1238–1247, doi:10.1242/jcs.044123.
[14] A. Carré, R.A.N. Louzada, R.S. Fortunato, R. Ameziane-El-Hassani, S. Morand, V. Ogryzko, D.P. de Carvalho, H. Grasberger, T.L. Leto, C. Dupuy, When an intramolecular disulfide bridge governs the interaction of DUOX2 with its partner DUOXA2, Antioxidants Redox Signal. 23 (2015) 724–733, doi:10.1089/ars.2015.6265.
[15] R.A. Louzada, R. Corre, R. Ameziane-El-Hassani, F. Hecht, J. Cazarin, C. Buffet, D.P. Carvalho, C. Dupuy, Conformation of the N-terminal ectodomain elicits different effects on DUOX function: a potential impact on congenital hypothyroidism caused by a H_2O_2 production defect, Thyroid 28 (2018) thy.2017.0596, doi:10.1089/thy.2017.0596.
[16] J.L. Meitzler, S. Hinde, B. Bánfi, W.M. Nauseef, P.R. Ortiz de Montellano, Conserved cysteine residues provide a protein-protein interaction surface in dual oxidase (DUOX) proteins, J. Biol. Chem. 288 (2013) 7147–7157, doi:10.1074/jbc.M112.414797.
[17] X. De Deken, D. Wang, J.E. Dumont, F. Miot, Characterization of ThOX proteins as components of the thyroid H_2O_2-generating system, Exp. Cell Res. 273 (2002) 187–196, doi:10.1006/excr.2001.5444.
[18] C. Hoste, J.E. Dumont, F. Miot, X. De Deken, The type of DUOX-dependent ROS production is dictated by defined sequences in DUOXA, Exp. Cell Res. 318 (2012) 2353–2364, doi:10.1016/j.yexcr.2012.07.007.
[19] T. Ueyama, M. Sakuma, Y. Ninoyu, T. Hamada, C. Dupuy, M. Geiszt, T.L. Leto, N. Saito, The extracellular A-loop of dual oxidases affects the specificity of reactive oxygen species release, J. Biol. Chem. 290 (2015) 6495–6506, doi:10.1074/jbc.M114.592717.
[20] X. De Deken, B. Corvilain, J.E. Dumont, F. Miot, Roles of DUOX-mediated hydrogen peroxide in metabolism, host defense and signaling, Antioxidants Redox Signal. 20 (2014) 2776–2793, doi:10.1089/ars.2013.5602.
[21] S. Rigutto, C. Hoste, H. Grasberger, M. Milenkovic, D. Communi, J.E. Dumont, B. Corvilain, F. Miot, X. De Deken, Activation of dual oxidases Duox1 and Duox2: differential regulation mediated by cAMP-dependent protein kinase and protein kinase C-dependent phosphorylation, J. Biol. Chem. 284 (2009) 6725–6734, doi:10.1074/jbc.M806893200.
[22] B. Bénard, J.-P. Brault, Production of peroxide in the thyroid, Union Med. Can. 100 (1971) 701–705.
[23] A. Botteaux, C. Hoste, J.E. Dumont, J. Van Sande, A. Allaoui, Potential role of Noxes in the protection of mucosae: H_2O_2 as a bacterial repellent, Microb. Infect. 11 (2009) 537–544, doi:10.1016/j.micinf.2009.02.009.
[24] C. Massart, C. Hoste, A. Virion, J. Ruf, J.E. Dumont, J. Van Sande, Cell biology of H_2O_2 generation in the thyroid: investigation of the control of dual oxidases (DUOX) activity in intact ex vivo thyroid tissue and cell lines, Mol. Cell. Endocrinol. 343 (2011) 32–44, doi:10.1016/j.mce.2011.05.047.
[25] M.C. Dinauer, E.A. Pierce, G.A.P. Bruns, J.T. Cumutte, S.H. Orkin, Human neutrophil cytochrome b light chain (p22-phox) - gene structure, chromosomal location, and mutations in cytochrome-negative autosomal recessive chronic granulomatous disease, J. Clin. Investig. 86 (1990) 1729–1737, doi:10.1172/JCI114898.
[26] M. Samson, A.L. Edinger, P. Stordeur, J. Rucker, M. Sharron, C. Govaerts, C. Mollereau, R.W. Doms, M. Parmentier, ChemR23, a putative chemoattractant receptor, is expressed in monocyte-derived dendritic cells and macrophages and is a coreceptor for SIV and some primary HIV-1 strains, Eur. J. Immunol. 28 (1998) 1689–1700, doi:10.1002/(SICI)1521-4141(199805)28:05<1689::AID-IMMU1689>3.0.CO;2-I.
[27] G.J. Graham, D6 and the atypical chemokine receptor family: novel regulators of immune and inflammatory processes, Eur. J. Immunol. 39 (2009) 342–351, doi:10.1002/eji.200838858.
[28] R. Ameziane-El-Hassani, M. Boufraqech, O. Lagente-Chevallier, U. Weyemi, M. Talbot, D. Métivier, F. Courtin, J.M. Bidart, M. El Mzibri, M. Schlumberger, C. Dupuy, Role of H_2O_2 in RET/PTC1 chromosomal rearrangement produced by ionizing radiation in human thyroid cells, Cancer Res. 70 (2010) 4123–4132, doi:10.1158/0008-5472.CAN-09-4336.
[29] R. Ameziane-El-Hassani, M. Talbot, M.C. de Souza Dos Santos, A. Al Ghuzlan, D. Hartl, J.-M. Bidart, X. De Deken, F. Miot, I. Diallo, F. de Vathaire, M. Schlumberger, C. Dupuy, NADPH oxidase DUOX1 promotes long-term persistence of oxidative stress after an exposure to irradiation, Proc. Natl. Acad. Sci. 112 (2015) 5051–5056, doi:10.1073/pnas.1420707112.
[30] N. Driessens, S. Versteyhe, C. Ghaddhab, A. Burniat, X. De Deken, J. Van Sande, J.E. Dumont, F. Miot, B. Corvilain, Hydrogen peroxide induces DNA single- and double-strand breaks in thyroid cells and is therefore a potential mutagen for this organ, Endocr. Relat. Cancer 16 (2009) 845–856, doi:10.1677/ERC-09-0020.
[31] K. Krohn, J. Maier, R. Paschke, Mechanisms of disease: hydrogen peroxide, DNA damage and mutagenesis in the development of thyroid tumors, Nat. Clin. Pract. Endocrinol. Metab. 3 (2007) 713–720, doi:10.1038/ncpendmet0621.
[32] Y. Song, N. Driessens, M. Costa, X. De Deken, V. Detours, B. Corvilain, C. Maenhaut, F. Miot, J. Van Sande, M.-C. Many, J.E. Dumont, Review: roles of hydrogen peroxide in thyroid physiology and disease, J. Clin. Endocrinol. Metab. 92 (2007) 3764–3773, doi:10.1210/jc.2007-0660.
[33] S. Versteyhe, N. Driessens, C. Ghaddhab, M. Tarabichi, C. Hoste, J.E. Dumont, F. Miot, B. Corvilain, V. Detours, Comparative analysis of the thyrocytes and T cells: responses to H_2O_2 and radiation reveals an H_2O_2-induced antioxidant transcriptional program in thyrocytes, J. Clin. Endocrinol. Metab. 98 (2013) E1645–E1654, doi:10.1210/jc.2013-1266.
[34] Y. Zhu, C.C. Marchal, A.-J. Casbon, N. Stull, K. Von Löhneysen, U.G. Knaus, A.J. Jesaitis, S. Mccormick, W.M. Nauseef, M.C. Dinauer, Deletion mutagenesis of p22 phox subunit of flavocytochrome b558, J. Biol. Chem. 281 (2006) 30336–30346, doi:10.1074/jbc.M607191200.
[35] H. Grasberger, X. De Deken, F. Miot, J. Pohlenz, S. Refetoff, Missense mutations of dual oxidase 2 (*DUOX2*) implicated in congenital hypothyroidism have impaired trafficking in cells reconstituted with DUOX2 maturation factor, Mol. Endocrinol. 21 (2007) 1408–1421, doi:10.1210/me.2007-0018.
[36] R.K. Ambasta, P. Kumar, K.K. Griendling, H.H.H.W. Schmidt, R. Busse, R.P. Brandes, Direct interaction of the novel Nox proteins with p22phox is required for the formation of a functionally active NADPH oxidase, J. Biol. Chem. 279 (2004) 45935–45941, doi:10.1074/jbc.M406486200.

[37] Y. Nakano, B. Bánfi, A.J. Jesaitis, M.C. Dinauer, L.-A.H. Allen, W.M. Nauseef, Critical roles for p22 phox in the structural maturation and subcellular targeting of Nox3, Biochem. J. 403 (2007) 97–108, doi:10.1042/BJ20060819.
[38] S. Lafranchi, Congenital Hypothyroidism: etiologies, diagnosis, and management, Thyroid 9 (1999) 735–740, doi:10.1089/thy.1999.9.735.
[39] S. Watanabe, C.S. Moniaga, S. Nielsen, M. Hara-Chikuma, Aquaporin-9 facilitates membrane transport of hydrogen peroxide in mammalian cells, Biochem. Biophys. Res. Commun. 471 (2016) 191–197, doi:10.1016/j.bbrc.2016.01.153.
[40] E.W. Miller, B.C. Dickinson, C.J. Chang, Aquaporin-3 mediates hydrogen peroxide uptake to regulate downstream intracellular signaling, Proc. Natl. Acad. Sci. 107 (2010) 15681–15686, doi:10.1073/pnas.1005776107.
[41] C. Ghaddhab, A. Kyrilli, N. Driessens, E. Van Den Eeckhaute, O. Hancisse, X. De Deken, J.E. Dumont, V. Detours, F. Miot, B. Corvilain, Factors contributing to the resistance of the thyrocyte to hydrogen peroxide, Mol. Cell. Endocrinol. 481 (2018) 62–70, doi:10.1016/j.mce.2018.11.010.
[42] J. Xiang, C. Wan, R. Guo, D. Guo, Is hydrogen peroxide a suitable Apoptosis inducer for all cell Types?, BioMed Res. Int. (2016) 1–6, doi:10.1155/2016/7343965.
[43] C. Marquer, S. Lévêque-Fort, M.-C. Potier, Determination of lipid raft partitioning of fluorescently-tagged probes in living cells by fluorescence correlation spectroscopy (FCS), J. Vis. Exp. 62 (2012) 1–8, doi:10.3791/3513.
[44] E.A. Ostrakhovitch, O.A. Semenikhin, p53-mediated regulation of neuronal differentiation via regulation of dual oxidase maturation factor 1, Neurosci. Lett. 494 (2011) 80–85, doi:10.1016/j.neulet.2011.02.061.